population expressed CD271/low-affinity nerve growth factor receptor (LNGFR) (Kanematsu et al. 2011).

In Vitro Multi lineage Differentiation

After 4 wk of chondrogenic differentiation, using a pellet culture system with dexamethasone (Dex), ascorbic acid 2-phosphate, sodium pyruvate, proline, recombinant human transforming growth factor-β3, and ITS+Premix (insulin, transferrin, selenious acid, linoleic acid) (Mackay et al. 1998, Lee et al. 2003), DMCs formed distinct cell pellets and expressed collagen type II alpha 1(COL2A1) protein, a chondrocyte differentiation-related marker, at a level similar to that seen in BM-MSCs (Fig. 9.4A). At the molecular level, quantitative reverse transcription-PCR (qRT-PCR) analysis showed that—as with BM-MSCs—levels of the master chondrogenesis regulator SRY-box 9 (SOX9) and the chondrocyte differentiation markers aggrecan (ACAN), COL2A1, and collagen type X alpha 1 (COL10A1) were significantly upregulated in DMCs after 4 wk in differentiation culture (Fig. 9.4A).

An adipogenic differentiation assay supplemented with Dex, 3-isobutyl-1-methylxanthine, indomethacin, recombinant human insulin, and 10 percent FBS (Zhang et al. 2004, Kanematsu et al. 2011) showed some oil red O staining of lipoidal substances in DMCs after 4 wk in differentiation culture; however, the amount was modest compared with that found in BM-MSCs (Fig. 9.4B). Levels of peroxisome proliferator—activated receptor gamma (PPARG), a master adipogenesis regulator, were significantly upregulated in DMCs, reaching the same level as found in BM-MSCs (Fig. 9.4B); however, the adipocyte differentiation markers adiponectin (ADIPOQ) and leptin (LEP) were not noticeably upregulated (Fig. 9.4B) (Kanematsu et al. 2011).

After 4 wk in osteogenic differentiation culture supplemented with Dex, β-glycerol phosphate, ascorbic acid 2-phosphate, and 10 percent FBS (Lee et al. 2003, Kanematsu et al. 2011), alizarin red S staining clearly showed calcium precipitate in BM-MSCs, indicating the cell-surface mineralization that characterizes osteogenic differentiation; no such staining was observed on the DMCs (Fig. 9.4C). Quantitative RT-PCR analysis showed that runt-related transcription factor 2 (RUNX2), a master osteogenesis regulator, was not upregulated in the DMCs (Fig. 9.4C). The osteoblast differentiation-related gene secreted protein acidic, cysteine-rich (SPARC; osteonectin) was significantly upregulated, but alkaline phosphatase (ALPL) and secreted phosphoprotein 1 (SPP1) were not (Fig. 9.4C). These findings showed that the multipotency differs between BM-MSCs and DMCs.

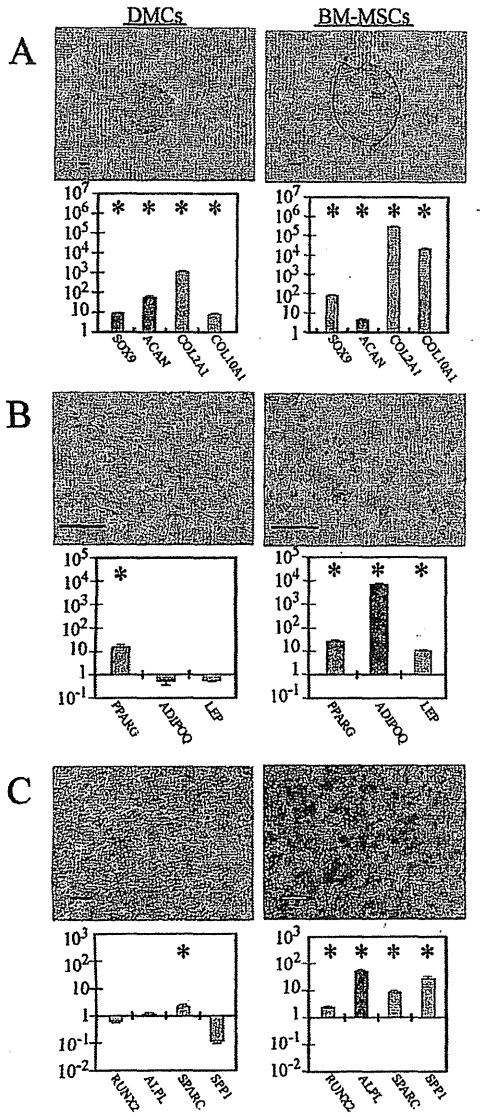

Figure 9.4 *In vitro* Multipotency of DMCs. DMCs were cultured for 63 DIV and passaged five times prior to the *in vitro* differentiation assays. BM-MSCs were cultured for 63 DIV and passaged seven times prior to the *in vitro* differentiation assays. Cultures were analyzed by immunohistochemistry and histological staining. Differentiation marker expression levels were measured by qRT-PCR and are expressed as fold change in expression levels compared with non-differentiated cultures (mean ± S.D., n=3). (A) Chondrogenic differentiation. Photographs show collagen type-II immunostaining results; bar graph shows relative expression levels of chondrocyte differentiation markers. (B) Adipogenic differentiation. Photographs show Oil red O staining results; bar graph shows relative expression levels of adipocyte differentiation markers. (C) Osteogenic differentiation. Photographs show Alizarin red S staining results; bar graphs show relative expression levels of osteogenic markers. *: $P<0.01$. Scale bar = 100 μm.

DMCs are of Purely Maternal Origin

Although it was possible that chorionic tissues were present at the boundary of the amnion or decidua when the DMCs were isolated, the genotypes of short tandem repeat (STR) polymorphisms clearly showed that all of the DMC genomic DNA samples examined had homozygous or heterozygous alleles of the 16 loci. None of the DMC-derived STR genotypes completely matched the genotypes of the amnion or UCB, which are derived from the fetus (Kanematsu et al. 2011). Furthermore, the location of the DMCs *in situ* was confirmed by immunohistochemistry of thinly sectioned fetal membrane tissue: vimentin-positive cells that did not express either HLA-G or CK19 (vimentin+/CK19-/HLA-G- cells) were found in the decidua vera, which lines the uterine wall (Kanematsu et al. 2011). These findings indicate that DMCs are of purely maternal origin.

The conclusions about the origin of MSCs isolated from fetal adnexal tissues in various studies have been mixed. Many studies concluded that the MSCs isolated from placental tissues were of fetal origin, although a thorough investigation was not carried out; a few reports clearly showed that isolated MSCs were of maternal origin (In 't Anker et al. 2004, Wulf et al. 2004, Barlow et al. 2008). Interestingly, some studies have reported that the genotype of placental MSCs is altered after several passages (Wulf et al. 2004, Soncini et al. 2007). Others reported that the proliferative capacity differs between cells of fetal versus maternal origin (In 't Anker et al. 2004, Kanematsu et al. 2011), and that some fetus-derived adherent cells, including amnion epithelial cells (AECs) and amnion mesenchymal cells (AMCs), grow and proliferate less vigorously than DMCs (Kanematsu et al. 2011).

Thus, although the cells isolated as MSCs from placental tissues might represent a heterogeneous population of both fetal and maternal origin when first cultured, the cells with the highest proliferative potential, such as DMCs, might form a homogeneous population with time in culture and with passaging, which selects for the fastest-growing population. The fetal and maternal contributions of placenta-derived MSCs must therefore be very carefully determined with the aid of genotyping or other highly sensitive, reproducible methods.

DMCs Have MSC-Like Properties but Differ from BM-MSCs

Many studies have reported isolating cells from fetal adnexa that were fibroblast-like, adherent, phenotypically similar to MSCs, and satisfied minimum MSC criteria (Table 9.1, 9.2) (Bailo et al. 2004, Fukuchi et al. 2004, Igura et al. 2004, In 't Anker et al. 2004, Wulf et al. 2004, Zhang et al. 2004, Li et al. 2005, Yen et al. 2005, Miao et al. 2006, Portmann-Lanz et al. 2006, Zhang et al. 2006, Alviano et al. 2007, Ilancheran et al. 2007, Battula

et al. 2007, Soncini et al. 2007, Sudo et al. 2007, Barlow et al. 2008, Stadler et al. 2008, Huang et al. 2009). Compared to these previously reported fetal adnexa-derived MSCs, DMCs have several unique and distinct cellular properties.

Multipotency

MSCs are usually defined as having tri-lineal multipotency, giving rise to osteogenic, adipogenic, and chondrogenic cells (Uccelli et al. 2008). However, several reports have indicated that the multipotency varies with the cell source (Table 9.1). DMCs differentiate readily into chondrocytes (Fig. 9.4A) (Kanematsu et al. 2011); similarly, MSCs derived from chorionic villi have good chondrogenic capability (Zhang et al. 2006). DMCs differentiate moderately well into adipocytes (Fig. 9.4B). MSCs derived from placenta or UCBs have low or no adipogenic capacity, in contrast to BM-MSCs or adipose tissue-derived MSCs (Barlow et al. 2008, Kern et al. 2006). In contrast, MSCs derived from human placental decidua basalis (PDB-MSCs) are reported to have multipotent differentiation potential (Huang et al. 2009). It was thought that DMCs might resemble PDB-MSCs, since their cell shape and oil-drop formation during adipogenic differentiation are very similar. The strong propensity of DMCs to differentiate into a chondrogenic lineage, and their modest ability to differentiate into the adipogenic lineage, might be characteristic of MSCs derived from extra-embryonic tissues. However, unlike BM-MSCs, DMCs show few osteogenic characteristics (Fig. 9.4C). A previous study showed that AECs had reduced osteogenic potential and an altered phenotype in culture (Stadler et al. 2008). Our modest culture length with a limited number of passages might have affected the differentiation potential of the DMCs, or their poor osteogenic capability might indicate a differentiation property specific to DMCs.

Careful observation is required to understand the multipotency of various MSCs. The appearance of the oil drops formed during adipogenesis was quite different between DMCs and BM-MSCs (Kanematsu et al. 2011). In BM-MSCs, the oil drops were large and accumulated in great quantity (Fig. 9.4B) (Pittenger et al. 1999, Kanematsu et al. 2011), while in DMCs, the oil drops were minute and scattered (Fig. 9.4B) (Kanematsu et al. 2011). In addition, the alteration of adipogenic-related markers in DMCs was marginal in comparison with that found in BM-MSCs (Fig. 9.4). Similar scattered, minute, adipogenesis-related oil drops were also described in PDB-MSCs and in other reports (Ilancheran et al. 2007, Portmann-Lanz et al. 2006, Soncini et al. 2007). The results of osteogenesis differentiation assays also require careful interpretation. The mineralization stained by alizarin red S or alkaline phosphatase activity usually covers the whole cell layer in BM-MSCs (Pittenger et al. 1999, Kanematsu et al. 2011). However, the

mineralization of MSCs derived from extra-embryonic tissues is reported to be limited or weak (Igura et al. 2004, Ilancheran et al. 2007, Li et al. 2005, Soncini et al. 2007). Taken together, these findings suggest that the differentiation capacity of DMCs has some similarities to that of MSCs, but differs substantially from that of BM-MSCs.

Cell-Surface Markers

MSC populations derived from various cell sources have universally shown similar cell-surface antigen patterns (Table 9.2). MSCs express CD29, CD44, CD49a-f, CD51, CD73, CD105, CD106, CD166, and Stro1, but do not express CD11b, CD14, CD45, or several others (Phinney and Prockop 2007). In addition, CD13 and CD90 have generally been used as positive MSC markers, and CD31, CD34, and CD133 as negative markers.

The expression pattern of cell-surface antigens on DMCs closely resembles that of BM-MSCs, with an interesting exception: a minor population of DMCs expresses CD45, which is present on all leukocytes and is therefore known as the leukocyte common antigen. Although MSCs are generally thought not to express CD45, several recent papers suggest that some non-hematopoietic and multi lineage stem cells do express it (Rogers et al. 2007, Kaiser et al. 2007). Low levels of CD45 are found on placenta-derived cells (Fukuchi et al. 2004); this vague expression of CD45 is similar on placenta-derived cells and DMCs. These findings suggest that DMCs are in fact a heterogeneous population containing a subpopulation of CD45-positive non-hematopoietic cells, like other placenta-derived cells. Since chondrogenic markers are enhanced in CD45-positive MSCs (Ahmed et al. 2006), a CD45-positive DMC subpopulation may contribute to robust chondrogenic differentiation.

Moreover, DMCs also express anti-fibroblast antigen, which is a surface membrane molecule expressed on human dermal fibroblasts (Singer et al. 1989). Several recent publications have shown that human fibroblasts derived from dermal skin have a multi lineage differentiation potential similar to that of BM-MSCs (Sudo et al. 2007, Lorenz et al. 2008). The presence of anti-fibroblast antigen on DMCs might indicate some type of correlation or biological similarity between DMCs and multipotent stem cells that exist in the skin.

Applications of DMCs in Regenerative Medicine

Practical Cell-Banking Systems

Among cells from fetal adnexal tissues, AECs and AMCs derived from the amnion are reported to have the least proliferative potential (Kanematsu

et al. 2011). Although these cells might have useful therapeutic effects, they are difficult to culture on any significant scale. While not superior to BM-MSCs in multipotency, DMCs have a better proliferative ability that should require less maintenance in cultivation. The derivation of DMCs from the maternal portion of the human fetal adnexal tissues, which are otherwise discarded, resolves many ethical concerns associated with the use of stem cells from human embryos or fetuses.

High success rates have been reported for isolating DMCs from tissues stored more than 24 hr in cool but not freezing temperatures; therefore, it may be feasible to develop a system for collecting or banking fetal adnexal tissue from multiple and even remote hospitals (Kanematsu et al. 2011). Although it cannot be said that the bacterial or fungal contamination rate is negligible in tissue samples obtained after vaginal delivery, the use of cesarean-delivered samples, or the institution of other quality controls, should reduce the pathogenic contamination and improve the quality of the DMCs obtained. Thus, DMCs are an excellent potential source of allogeneic MSCs for regenerative medicine, and a cell banking system designed for DMCs is worth considering.

PeriCellular Matrix of Decidua-derived Mesenchymal Cells (PCM-DM) is a Potent Human-Derived Substrate for Human Pluripotent Stem Cell Maintenance Culture

Unlike mouse embryonic stem cells, hESCs and hiPSCs are maintained on either living feeder cells, such as mouse embryonic fibroblasts (MEFs) (Thomson et al. 1998, Reubinoff et al. 2000, Takahashi et al. 2007), or on Matrigel or another special culture substrate (Xu et al. 2001). However, to expand the clinical potential of hESCs and hiPSCs, the use of animal-derived materials in the culture should be minimized to avoid animal-related allergic risks and pathogens (Martin et al. 2005). Thus, the clinical application of hESCs and hiPSCs requires an alternative human-origin substrate. PCM-DM is able to support hESC and hiPSC growth and pluripotency (Nagase et al. 2009), and a feeder-free system using PCM-DM promises to be a practical method for culturing hESCs and hiPSCs for clinical applications.

PCM-DM is prepared from DMCs cultured on gelatin-coated plastic dishes and lysed by deoxycholate (Fig. 9.5A) (Nagase et al. 2009). PCM-DM has been shown to support hESC culture in MEF-conditioned medium (MEF-CM). PCM-DM supported the growth of hESCs with an efficiency similar to, or slightly better than that of Matrigel, an animal-derived substrate, in MEF-CM (Nagase et al. 2009). PCM-DM-based culture is compatible with non-conditioned commercial defined medium, for instance Invitrogen's StemPro hESC SFM, and is capable of maintaining dissociated

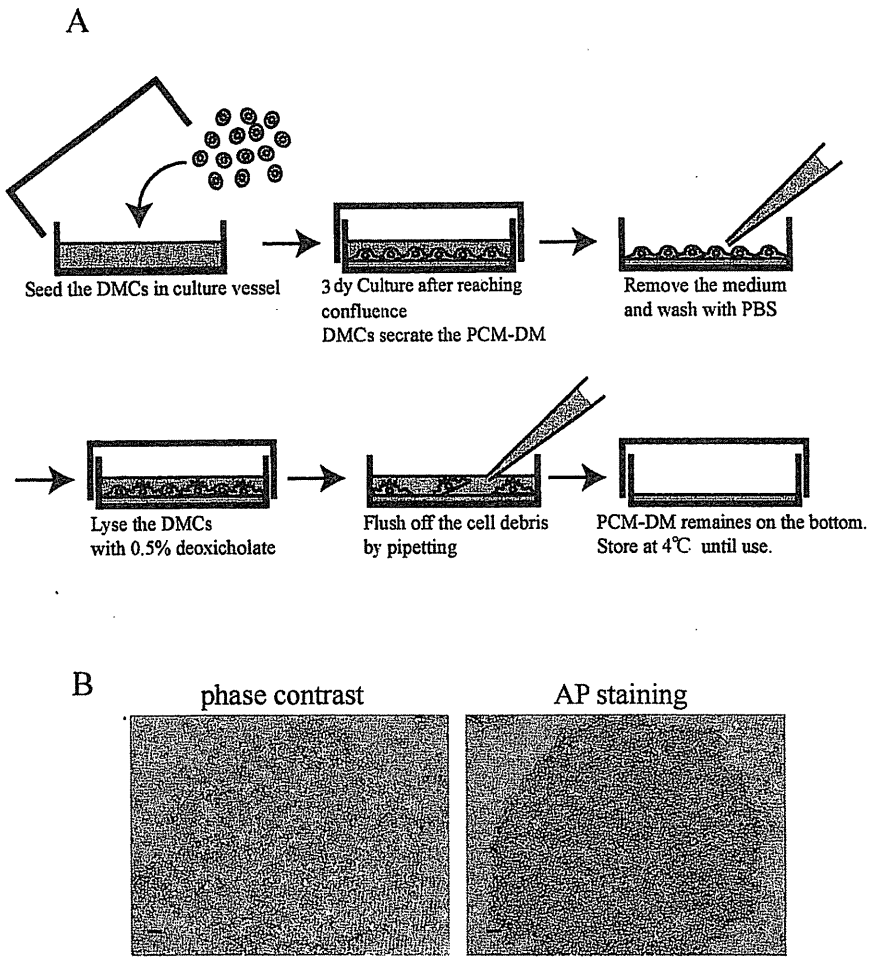

Figure 9.5 PeriCellular Matrix of Decidua-derived Mesenchymal cells (PCM-DM) Applications for hESC and hiPSC Culture. (A) Schematic: Preparation of PCM-DM as a substrate for feeder-free hESC or hiPSC culture. (B) Human iPSCs (201B7 line) cultured on PCM-DM without feeder cells. Left: phase-contrast image. Right: alkaline phosphatase activity. Scale bar = 100 μm.

hESCs. Human ESCs maintained on PCM-DM in StemPro retain their *in vitro* and *in vivo* pluripotency after multiple passages (Nagase et al. 2009). Notably, PCM-DM's ability to support maintenance culture is very stable and can be preserved for at least 8 mon after preparation by keeping the plate refrigerated under semi-dry conditions. Moreover, PCM-DM is suitable for hiPSC maintenance culture (Fig. 9.5B), and supports hiPSC growth as efficiently as Matrigel (Nagase et al. 2009).

Since DMCs can be prepared and expanded in large quantities, PCM-DM is a practical human-derived alternative to the animal-derived substrates currently in use for clinical-grade hESC and hiPSC culture.

A Cell Source for Generating hiPSCs

Human somatic cells can be reprogrammed into iPSCs by the forced transduction of Oct4, Sox2, Klf4, and c-Myc (Takahashi et al. 2007). These iPSCs closely resemble ESCs in their gene expression pattern and epigenetic profile, and the transduced transcription factors restore iPSC pluripotency both *in vitro* and *in vivo*. Regenerative treatments that use patient-derived autologous somatic stem cells or iPSCs are the most desirable, from both a safety and ethical perspective. We anticipate that human iPSCs will contribute substantially to making the clinical use of autologous pluripotent stem cells a reality. The transplantation of allogeneic human somatic stem cells derived from hESCs or hiPSCs is also a promising approach, especially for treating acute diseases or injuries such as stroke or spinal cord injury, in which cells must be transplanted during the acute to sub-acute stage.

Besides being an attractive source of allogeneic MSCs, DMCs are a potential cell source for generating hiPSCs. DMCs can be reprogrammed into hiPSCs (DMC-hiPSCs) using retroviral reprogramming-factor gene transfers (Kanemura 2010, Shofuda et al. 2012). DMC-hiPSCs have characteristics equivalent to hESCs in colony morphology (Fig. 9.6), global gene expression profile including human pluripotent stem cell markers, DNA methylation status of OCT3/4 and NANOG promoters, and the ability to differentiate into components of three germ layers *in vitro* as well as *in vivo* (Shofuda et al. 2012).

Moreover, PCM-DM is a practical, versatile human substrate for both the feeder-free generation and the stable long-term maintenance of hiPSCs (Fukusumi et al., submitted). These unique properties of DMCs offer several advantages for clinical use, not only as an attractive alternative to allogeneic MSCs for regenerative medicine, but also as a practical contributor in hiPSC-banking systems, which will increase the feasibility of using allogeneic stem cells for clinical applications (Kanemura 2010).

Ethical Advantages of Fetal Adnexa-Derived DMCs

Since fetal adnexal tissues must inevitably be dealt with in association with childbirth, obtaining samples does not require surgery or invasive procedures, or entail additional pain or risk for the donor. This alone makes fetal adnexal tissue an advantageous source of allogeneic human cells. The maternal, rather than fetal, origin of DMCs also has significant advantages. Consent to the clinical use of samples can be obtained from the donor

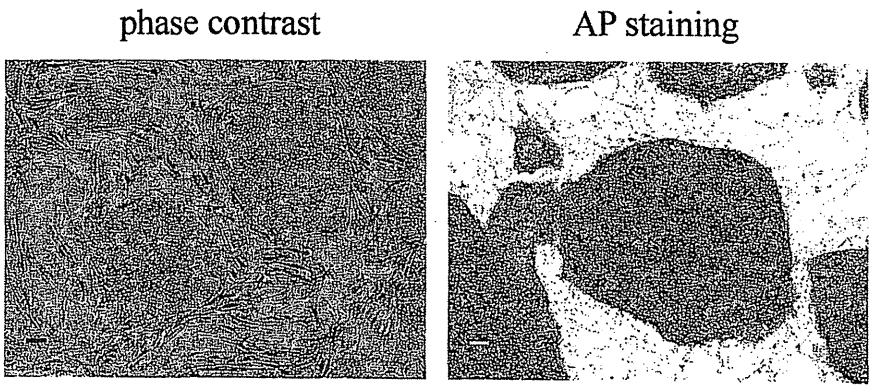

Figure 9.6 Human iPSCs Generated from DMCs. Left: phase-contrast image of DMC-derived human iPSC colonies cultured on MEF feeder. Right: alkaline phosphatase activity. Scale bar = 100 μm.

directly, which is especially important when using human allogeneic cells or tissues for medical purposes. Screening donors' clinical history and health, especially with regard to infectious or inherited diseases, is indispensable; here again, the maternal origin of DMCs makes it feasible to examine the donor's condition and history with her consent. In view of developing the large-scale processing and availability of human cells, tissues, and cell- and tissue-based products (HCT/Ps), DMCs have significant advantages without the ethical and medical issues associated with fetal-derived cell sources, reducing both the potential risks and costs of making HCT/Ps available for clinical use.

Conclusions

Many researchers have reported the successful isolation of MSCs from fetal adnexal tissue, a promising new source of cells for regenerative medicine. Among these, DMCs, which are MSCs isolated from the term decidua vera, are of special interest. DMCs have a typical fibroblast-like morphology, high proliferative potential lasting through more than 30 population doublings, good *in vitro* differentiation into chondrocytes, and moderate differentiation into adipocytes—although unlike BM-MSCs, DMCs show little evidence of osteogenesis. It has been demonstrated that hiPSCs can be efficiently generated from DMCs. PCM-DM is a potent and versatile non-animal substrate material capable of supporting feeder-free culture and generating hESCs and hiPSCs. These unique properties of DMCs resolve many ethical concerns associated with the use of hESCs and hiPSCs and offer significant advantages for their clinical use.

Acknowledgments

We would like to express our gratitude to Dr. Chiaki Ban, Dr. Mami Yamasaki, and Ms. Chika Teramoto at the Osaka National Hospital, and to all of the members of our laboratory. These studies were supported by the Project for the Realization of Regenerative Medicine (the research field for the development of stem cell therapy) from the Ministry of Education, Culture, Sports, Science and Technology (MEXT) of Japan, and by the Cooperative Link of Unique Science and Technology for Economy Revitalization (CLUSTER) project from MEXT, Japan.

References

Ahmed, N., B. Vogel, E. Rohde, D. Strunk, J. Grifka, M.B. Schulz and S. Grässel. 2006. CD45-positive cells of hematopoietic origin enhance chondrogenic marker gene expression in rat marrow stromal cells. Int. J. Mol. Med. 18: 233–240.

Alviano, F., V. Fossati, C. Marchionni, M. Arpinati, L. Bonsi, M. Franchina, G. Lanzoni, S. Cantoni, C. Cavallini, F. Bianchi, P.L. Tazzari, G. Pasquinelli, L. Foroni, C. Ventura, A. Grossi and G.P. Bagnara. 2007. Term amniotic membrane is a high throughput source for multipotent mesenchymal stem cells with the ability to differentiate into endothelial cells *in vitro*. BMC Dev. Biol. 7: 11.

Bailo, M., M. Soncini, E. Vertua, P.B. Signoroni, S. Sanzone, G. Lombardi, D. Arienti, F. Calamani, D. Zatti, P. Paul, A. Albertini, F. Zorzi, A. Cavagnini, F. Candotti, G.S. Wengler and O. Parollini. 2004. Engraftment potential of human amnion and chorion cells derived from term placenta. Transplantation. 78: 1439–1448.

Barlow, S., G. Brooke, K. Chatterjee, G. Price, R. Pelekanos, T. Rossetti, M. Doody, D. Venter, S. Pain, K. Gilshenan and K. Atkinson. 2008. Comparison of human placenta- and bone marrow-derived multipotent mesenchymal stem cells. Stem Cells Dev. 17: 1095–1108.

Battula, V.L., P.M. Bareiss, S. Treml, S. Conrad, I. Albert, S. Hojak, H. Abele, B. Schewe, L. Just, T. Skutella and H.J. Bühring. 2007. Human placenta and bone marrow derived MSC cultured in serum-free, b-FGF-containing medium express cell surface frizzled-9 and SSEA-4 and give rise to multilineage differentiation. Differentiation. 75: 279–291.

Bretzner, F., F. Gilbert, F. Baylis and R.M. Brownstone. 2011. Target populations for first-in-human embryonic stem cell research in spinal cord injury. Cell Stem Cell. 8: 468–475.

Caplan, A.I. 1991. Mesenchymal stem cells. J. Orthop. Res. 9: 641–650.

Dominici, M., K.L. Blanc, I. Mueller, I. Slaper-Cortenbach, F.C. Marini, D.S. Krause, R.J. Deans, A. Keating, D.J. Prockop and E.M. Horwitz. 2006. Minimal criteria for defining multipotent mesenchymal stromal cells. The International Society for Cellular Therapy Position Statement. Cytotherapy. 8: 315–317.

Fukuchi, Y., H. Nakajima, D. Sugiyama, I. Hirose, T. Kitamura and K. Tsuji. 2004. Human placenta-derived cells have mesenchymal stem/progenitor cell potential. Stem Cells 22: 649–658.

Goldman, S. 2005. Stem and progenitor cell-based therapy of the human central nervous system. Nat. Biotechnol. 23: 862–871.

Horwitz, E.M., K.L .Blanc, M. Dominici, I. Mueller, I. Slaper-Cortenbach, F.C. Marini, R.J. Deans, D.S. Krause and A. Keating. 2005. Clarification of the nomenclature for MSC: The International Society for Cellular Therapy Position Statement. Cytotherapy. 7: 393–395.

Huang, Y.C., Z.M. Yang, X.H. Chen, M.Y. Tan, J. Wang, X.Q. Li, H.Q. Xie and L. Deng. 2009. Isolation of mesenchymal stem cells from human placental decidua basalis and resistance to hypoxia and serum deprivation. Stem Cell Rev. Rep. 5: 247–255.

Igura, K., X. Zhang, K. Takahashi, A. Mitsuru, S. Yamaguchi and T.A. Takahashi. 2004. Isolation and characterization of mesenchymal progenitor cells from chorionic villi of human placenta. Cytotherapy. 6: 543–553.

Ilancheran, S., A. Michalska, G. Peh, E.M. Wallace, M. Pera and U. Manuelpillai. 2007. Stem cells derived from human fetal membranes display multilineage differentiation potential. Biol. Reprod. 77: 577–588.

Ilancheran, S., Y. Moodley and U. Manuelpillai. 2009. Human fetal membranes: a source of stem cells for tissue regeneration and repair? Placenta. 30: 2–10.

In 't Anker, P.S., S.A. Scherjon, C. Kleijburg-van der Keur, G.M.J.S. De Groot-Swings, F.H.J. Class, W.E. Fibbe and H.H.H. Kanhai. 2004. Isolation of mesenchymal stem cells of fetal or maternal origin from human placenta. Stem Cells. 22: 1338–1345.

Kaiser, S., B. Hackanson, M. Follo, A. Mehlhorn, K. Geiger, G. Ihorst and U. Kapp. 2007. BM cells giving rise to MSC in culture have a heterogeneous CD34 and CD45 phenotype. Cytotherapy. 9: 439–450.

Kanematsu, D., T. Shofuda, A. Yamamoto, C. Ban, T. Ueda, M. Yamasaki and Y. Kanemura. 2011. Isolation and cellular properties of mesenchymal cells derived from the decidua of human term placenta. Differentiation. 82: 77–88.

Kanemura, Y. 2010. Development of cell-processing systems for human stem cells (neural stem cells, mesenchymal stem cells, and iPS cells) for regenerative medicine. Keio J. Med. 59: 35–45.

Kern, S., H. Eichler, J. Stoeve, H. Klüter and K. Bieback. 2006. Comparative analysis of mesenchymal stem cells from bone marrow, umbilical cord blood, or adipose tissue. Stem Cells. 24: 1294–1301.

Koch, P., Z. Kokaia, O. Lindvall and O. Brüstle. 2009. Emerging concepts in neural stem research: autologous repair and cell-based disease modelling. Lancet Neurol. 8: 819–829.

Koide, Y., S. Morikawa, Y. Mabuchi, Y. Muguruma, E. Hiratsu, K. Hasegawa, M. Kobayashi, K. Ando, K. Kinjo, H. Okano and Y. Matsuzaki. 2007. Two distinct stem cell lineages in murine bone marrow. Stem Cells. 25: 1213–1221.

Lee, H.S., G.T. Huang, H. Chiang, L.L. Chiou, M.H. Chen, C.H. Hsieh and C.C. Jiang. 2003. Multipotential mesenchymal stem cells from femoral bone marrow near the site of osteonecrosis. Stem Cells. 21: 190–199.

Li, C.D., W.Y. Zhang, H.L. Li, X.X. Jiang, Y. Zhang, P. Tang and N. Mao. 2005. Mesenchymal stem cells derived from human placenta suppress allogenic umbilical cord blood lymphocyte proliferation. Cell Res. 15: 539–547.

Lorenz, K., M. Sicker, E. Schmelzer, T. Rupf, J. Salvetter, M. Schulz-Siegmund and A. Bader. 2008. Multilineage differentiation potential of human dermal skin-derived fibroblasts. Exp. Dermatol. 17: 925–932.

Mackay, A.M., S.C. Beck, J.M. Murphy, F.P. Barry, C.O. Chichester and M.F. Pittenger. 1998. Chondrogenic differentiation of cultured human mesenchymal stem cells from marrow. Tissue Eng. 4: 415–428.

Marcus, A.J. and D. Woodbury. 2008. Fetal stem cells from extra-embryonic tissues: do not discard. J. Cell. Mol. Med. 12: 730–742.

Martin, M., A. Muotri, F. Gage and A. Varki. 2005. Human embryonic stem cells express an immunogenic nonhuman sialic acid. Nat. Med. 11: 228–232.

Miao, Z., J. Jin, L. Chen, J. Zhu, W. Huang, J. Zhao, H. Qian and X. Zhang. 2006. Isolation of mesenchymal stem cells from human placenta: comparison with human bone marrow mesenchymal stem cells. Cell Biol. Int. 30: 681–687.

Nagase, T., M. Ueno, M. Matsumura, K. Muguruma, M. Ohgushi, N. Kondo, D. Kanematsu, Y. Kanemura and Y. Sasai. 2009. Pericellular matrix of decidua-derived mesenchymal cells: a potent human-derived substrate for the maintenance culture of human ES cells. Dev. Dyn. 238: 1118–1130.

Parolini, O., G. Alviano, G.P. Bagnara, G. Bilic, H.J. Bühring, M. Evangelista, S. Hennerbichler, B. Liu, M. Magatti, N. Mao, T. Miki, F. Marongiu, H. Nakajima, T. Nikaido, C.B.P. Lanz, V. Sankar, M. Soncini, G. Stadler, D. Surbek, T.A. Takahashi, H. Redl, N. Sakuragawa, S. Wolbank, S. Zeisberger, A. Zisch and S.C. Strom. 2008. Concise review: isolation and characterization of cells from human term placenta: outcome of the first international workshop on placenta derived stem cells. Stem Cells. 26: 300–311.

Phinney, D.G. and D.J. Prockop. 2007. Concise Review: Mesenchymal stem/multipotent stromal cells: the state of transdifferentiation and modes of tissue repair—Current views. Stem Cells. 25: 2896–2902.

Pittenger, M.F., A.M. Mackay, S.C. Beck, R.K. Jaiswal, R. Douglas, J.D. Mosca, M.A. Moorman, D.W. Simonetti, S. Craig and D.R. Marshak. 1999. Multilineage potential of adult human mesenchymal stem cells. Science. 284: 143–147.

Portmann-Lanz, C.B., A. Schoeberlein, A. Huber, R. Sager, A. Malek, W. Holzgreve and D.V. Surbek. 2006. Placental mesenchymal stem cells as potential autologous graft for pre- and perinatal neuroregeneration. Am. J. Obstet. Gynecol. 194: 664–673.

Reubinoff, B.E., M.F. Pera, C.Y. Fong, A. Trounson and A. Bonfso. 2000. Embryonic stem cell lines from human blastocysts: somatic differentiation *in vitro*. Nat. Biotechnol. 18: 399–404.

Rogers, I., N. Yamanaka, R. Bielecki, C.J. Wong, S. Chua, S. Yuen and R.F. Casper. 2007. Identification and analysis of *in vitro* cultured CD45-positive cells capable of multi-linage differentiation. Exp. Cell Res. 313: 1839–1852.

Shofuda, T., D. Kanematsu, H. Fukusumi, A. Yamamoto, Y. Bamba, S. Yoshitatsu, H. Suemizu, M. Nakamura, Y. Sugimoto, M.K. Furue, A. Kohara, W. Akamatsu, Y. Okada, H. Okano, M. Yamasaki and Y. Kanemura. 2012. Human Decidua-Derived Mesenchymal Cells are a Promising Source for the Generation and Cell Banking of Human Induced Pluripotent Stem Cells. Cell Med. (in press).

Singer, K.H., R.M. Scearce, D.T. Tuck, L.P. Whichard, S.M. Denning and B.F. Haynes. 1989. Removal of fibroblasts from human epithelial cell cultures with use of a complement fixing monoclonal antibody reactive with human fibroblasts and monocytes/macrophages. J. Invest. Dermtol. 92: 166–170.

Soncini, M., E. Vertua, L. Gibelli, F. Zorzi, M. Denegri, A. Albertini, G.S. Wengler and O. Parolini. 2007. Isolation and characterization of mesenchymal cells from human fetal membranes. J. Tissue Eng. Regener. Med. 1: 296–305.

Stadler, G., S. Hennerbichler, A. Lindenmair, A. Peterbauer, K. Hofer, M. van Griensven, C. Gabriel, H. Redl and S. Wolbank. 2008. Phenotypic shift of human amniotic epithelial cells in culture is associated with reduced osteogenic differentiation *in vitro*. Cytotherapy. 10: 743–752.

Sudo, K., M. Kannno, K. Miharada, S. Ogawa, T. Hiroyama, K. Saijo and Y. Nakamura. 2007. Mesenchymal progenitors able to differentiate into osteogenic, chondrogenic, and/or adipogenic cells *in vitro* are present in most primary fibroblast-like cell populations. Stem Cells. 25: 1610–1617.

Takahashi, K., K. Tanabe, M. Ohnuki, M. Narita, T. Ichikawa, K. Tomoda and S. Yamanaka. 2007. Induction of pluripotent stem cells from adult human fibroblasts by defined factors. Cell. 131: 861–872.

Thomson, J.A., J.I. Eldor, S.S. Shapiro, M.A. Waknitz, J.J. Swiergiel, V.S. Marshall and J.M. Jones. 1998. Embryonic stem cell lines derived from human blastocysts. Science. 282: 1145–1147.

Uccelli, A., L. Moretta and V. Pistoia. 2008. Mesenchymal stem cells in health and disease. Nat. Rev. Immunol. 8: 726–736.

Wulf, G.G., V. Viereck, B. Hemmerlein, D. Haase, K. Vehmeyer, T. Pukrop, B. Glass, G. Emons and L. Trümper. 2004. Mesengenic progenitor cells derived from human placenta. Tissue Eng. 10: 1136–1147.

Xu, C., M.S. Inokuma, J. Denham, K. Golds, P. Kundu, J.D. Gold and M.K. Carpenter. 2001. Feeder-free growth of undifferentiated human embryonic stem cells. Nat. Biotechnol. 19: 971–974.

Yen, B.L., H.I. Huang, C.C. Chien, H.Y. Jui, B.S. Ko, M. Yao, C.T. Shun, M.L. Yen, M.C. Lee and Y.C. Chen. 2005. Isolation of multipotent cells from human term placenta. Stem Cells. 23: 3–9.

Zhang, X., A. Mitsuru, K. Igura, K. Takahashi, S. Ichinose, S. Yamaguchi and T.A. Takahashi. 2006. Mesenchymal progenitor cells derived from chorionic villi of +human placenta for cartilage tissue engineering. Biochem. Biophys. Res. Commun. 340: 944–952.

Zhang, Y., C. Li, X. Jiang, S. Zhang, Y. Wu,'B. Liu, P. Tang and N. Mao. 2004. Human placenta-derived mesenchymal progenitor cells support culture expansion of long-term culture-initiating cells from cord blood CD34+ cells. Exp. Hematol. 32: 657–664.

CLINICAL REPORT

AMERICAN JOURNAL OF medical genetics PART A

Hydrocephalus With Hirschsprung Disease: Severe End of X-linked Hydrocephalus Spectrum

Toshiki Takenouchi,[1] Mie Nakazawa,[2] Yonehiro Kanemura,[3,4] Sachiko Shimozato,[1] Mami Yamasaki,[4,5] Takao Takahashi,[1] and Kenjiro Kosaki[1,6]*

[1]Department of Pediatrics, Keio University School of Medicine, Tokyo, Japan

[2]Department of Pediatrics, Tokyo Metropolitan Ohtsuka Hospital, Tokyo, Japan

[3]Division of Regenerative Medicine, Institute for Clinical Research, Osaka National Hospital, National Hospital Organization, Osaka, Japan

[4]Department of Neurosurgery, Osaka National Hospital, National Hospital Organization, Osaka, Japan

[5]Division of Molecular Medicine, Institute for Clinical Research, Osaka National Hospital, National Hospital Organization, Osaka, Japan

[6]Center for Medical Genetics, Keio University School of Medicine, Tokyo, Japan

Received 25 August 2011; Accepted 26 December 2011

L1CAM molecule is a cell adhesion molecule in nervous and enteric systems and is responsible for X-linked hydrocephalus (XLH) spectrum, which is a rare condition with severe congenital hydrocephalus, dysgenesis of the corpus callosum, intellectual disability, spasticity, and adducted thumbs. Several cases of XLH accompanied by Hirschsprung disease (HSCR) have been reported in the literature, but whether HSCR results from a gain-of-function mutation in cases with XLH, i.e., a neomorphic mutation, or the severe end of the *L1CAM* mutation spectrum remains unclear. The present patient was a Japanese boy with severe congenital hydrocephalus with aqueductal stenosis as well as hypoplasia of the corpus callosum. HSCR had been confirmed by a biopsy. A mutation analysis of the *L1CAM* gene showed a C61T mutation in exon 1, resulting in a truncating nonsense mutation at amino acid position 21 and producing an extremely short protein that was unlikely to interact with other proteins. These findings suggest that XLH-HSCR represents the severe end of the XLH spectrum, rather than a neomorphic mutation. A thorough abdominal investigation to rule out HSCR should be considered in patients with XLH accompanied by severe constipation.

Key words: hydrocephalus; Hirschsprung disease; neural cell adhesion molecule L1

How to Cite this Article:
Takenouchi T, Nakazawa M, Kanemura Y, Shimozato S, Yamasaki M, Takahashi T, Kosaki K. 2012. Hydrocephalus with Hirschsprung disease: Severe end of X-linked hydrocephalus spectrum.
Am J Med Genet Part A 158A:812–815.

INTRODUCTION

The L1 cell adhesion molecule [L1CAM, OMIM 308840] is expressed primarily in the central nervous system and represents an important component of the ligand–receptor network of guidance forces that influence axonal growth and guidance [Kenwrick et al., 2000]. Reflecting its expression pattern, mutations in the L1CAM gene, located at Xq28, lead to an X-linked hydrocephalus (XLH) spectrum characterized by severe congenital hydrocephalus accompanied by intellectual disability, spasticity, and thumb flexion over the palm [Jones, 2006]. Recently, L1CAM was shown to be expressed by neural crest cells as they colonize the developing gut in mice [Anderson et al., 2006].

Not unexpectedly, the association of XLH and Hirschsprung disease (HSCR) has been observed in several cases [Okamoto et al., 1997, 2004; Vits et al., 1998; Parisi et al., 2002; Basel-Vanagaite et al., 2006; Nakakimura et al., 2008; Griseri et al., 2009; Jackson et al., 2009]. So far, the classes of mutation found in patients with XLH and HSCR included missense and truncating mutations devoid of an intracellular domain. The mechanistic basis by which the additional phenotype, i.e., HSCR, arises from these classes of mutations, has been unclear. Two mechanisms can be considered: first, the feature, i.e., HSCR, might represent the result of a gain-of-function mutation in that HSCR is an additive but atypical feature of XLH. Hence, HSCR could be interpreted as a "neomorphic" mutation from a structural standpoint and may represent a "gain-of-function" mutation from a functional standpoint. In support of

Abbreviations: L1CAM, L1 cell adhesion molecule; HSCR, Hirschsprung disease; XLH, X-linked hydrocephalus.

*Correspondence to:
Kenjiro Kosaki, MD, Center for Medical Genetics, Keio University School of Medicine, 35 Shinanomachi, Shinjuku, Tokyo, 1608582 Japan.
E-mail: kkosaki@z3.keio.jp

Published online 21 February 2012 in Wiley Online Library (wileyonlinelibrary.com).
DOI 10.1002/ajmg.a.35245

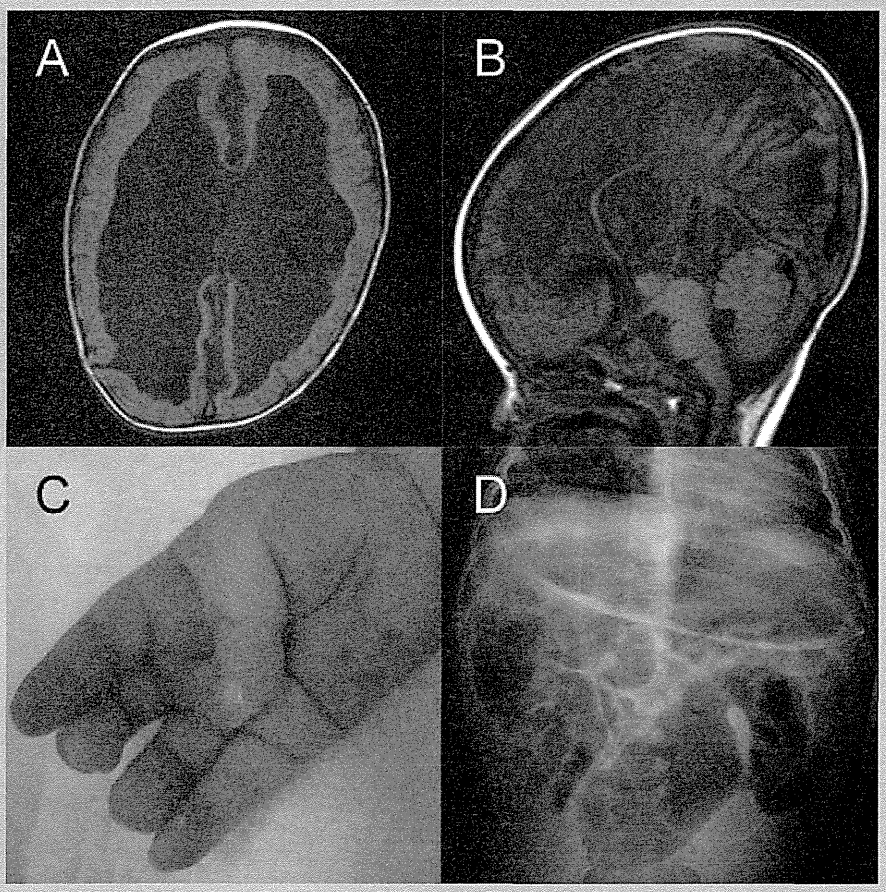

FIG. 1. Clinical and radiographic characteristics of the propositus. Magnetic resonance imaging of the brain at 11 months of age (after ventriculoperitoneal shunt placement) showed a significant dilatation of the lateral ventricles (A) and dysgenesis of the corpus callosum (B). Spontaneous adduction of the thumbs was also noted (C). An abdominal X-ray obtained at 17months of age (after surgical correction) showed a marked dilation of the colorectal bowel loop, consistent with HSCR (D).

this "gain-of-function" mutation hypothesis, the L1CAM protein functions as a hetero-multimer with other proteins, such as TAG-1. Presently known classes of mutations including missense and truncating mutations devoid of an intracellular domain are not incompatible with this hypothesis. Alternatively, XLH-HSCR may represent the severe end of the L1CAM mutation spectrum, in which the morphogenesis of both the central nervous system and the neural crest-derived system, i.e., enteric neurons, are affected.

CLINICAL REPORT

The propositus is a Japanese boy born to nonconsanguineous parents. There was no family history of known inherited genetic conditions or HSCR. A prenatal ultrasound diagnosed the propositus as having hydrocephalus at 28 weeks of gestation. An amniocentesis revealed a normal karyotype of 46, XY. He was born at 37 and 3/7 weeks of gestation with a birth weight of 3,088 g. Magnetic resonance imaging of the brain demonstrated severe hydrocephalus with aqueductal stenosis as well as hypoplasia of the corpus callosum (Fig. 1A and B). A ventriculoperitoneal shunt was placed at the age of 15 days for the treatment of the severe and progressive hydrocephalus. Since he had severe constipation and abdominal distention, a rectal biopsy was performed at age 13 days. The biopsy showed the absence of rectal ganglion cells, confirming a diagnosis of HSCR. He underwent surgical resection and reconstruction of the internal anal sphincter muscle at age 43 days. Postoperatively, he was noted to have hydronephrosis with subsequent frequent urinary tract infections. Given his characteristic facial features with frontal bossing and adducted thumbs (Fig. 1C) and severe developmental delay, a mutation analysis for the L1CAM gene was performed. L1CAM is composed of six immunoglobulin superfamily domains followed by five fibronectin type III domains, a single-pass transmembrane region, and a cytoplasmic domain [Bateman et al., 1996]. The mutation analysis of our patient demonstrated a C61T mutation in exon 1 with a resultant truncating nonsense mutation at amino acid position 21

TABLE I. Reported Patients of XLH Spectrum and HSCR with Pathological *L1CAM* Mutations

Case #	References	Mutations		Consequence	Domain	Class of mutations	Age at diagnosis	Severe hydrocephalus	Ventriculo-peritoneal shunt placement	Cerebellar hypoplasia	Dysgenesis of CC	HSCR	Adducted thumbs	Mental retardation	Urogenital Abnormalities
1	Okamoto et al., 1997	2421delTG	Exon 18	Nonsense	Fn III-2	III	25 wks GA	+	+	+	+	+	+	+	NR
2	Vits et al., 1998; Case 1	G1895C	Exon 15	R632P	Fn III-1	II-Key	After birth	+	NR	+	+	+	+	+	NR
3	Parisi et al., 2002	G2254A	Exon 18	V752M	Fn III-2	II-Key	23 wks GA	+	+	NR	+	+	+	+	+[a]
4	Okamoto et al., 2004; Case 1	IVS15+5G->A	Intron15	NR	NR	Splice donor-site	After birth	+	NR	+	+	+	+	NR	NR
5	Case 2	IVS15+5G->A	Intron15	NR	NR	Splice donor-site	17 wks GA	+	+	+	+	+	+	NR	NR
6	Case 3	C2974T	Exon 22	Q992X	Fn III-4	III	After birth	+	NR	NR	+	+	+	+	NR
7	Basel-Vanagaite et al., 2006; Case 1	C719T	Exon7	P240L	Ig-3	II-Key	24 wks GA	–	NR	+	+	+	–	+	NR
8	Case 2	C719T	Exon7	P240L	Ig-3	II-Key	24 wks GA	–	NR	+	+	+	–	+	NR
9	Nakakimura et al., 2008	T92C	Exon 3	V31A	Above Ig-1	II-non Key	28 wks GA	+	+	NR	+	+	+	NR	NR
10	Jackson et al., 2009	NR	Exon 13	R558X	Ig-6	III	3rd trimester	+	+	NR	NR	+	+	NR	NR
11	Griseri et al., 2009	2265delC	Exon 18	P756L fs95X	Fn III-2	III	after birth	+	+	NR	NR	+	+	+	[b]
12	The propositus	C61T	Exon 1	Q21X	Above Ig-1	III	28 wks GA	+	+	+	+	+	+	+	[c]

CC, corpus callosum; GA, gestational age; Fn, fibronectin; HSCR, Hirschsprung disease; Ig, immunoglobulin; Classes of mutations [Yamasaki et al., 1997]; I: mutations that affect only the cytoplasmic domain of L1 molecule; II: missense mutations in the extracellular domain; III: nonsense or frame shift mutations that produce a premature stop codon in the extracellular domain.
Key, involvement of "key" amino acid residues [Bateman et al., 1996]; NR, not recorded.

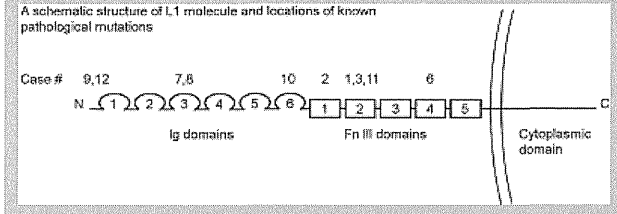

[a]Micropenis, a small descended testis and a cryptorchid left testis.
[b]Vesicourethral reflux and frequent urinary tract infections.
[c]Postoperative frequent urinary tract infections without vesicoureteral reflux.

(i.e., Q21X) causing a near-complete deletion of the L1CAM molecule.

DISCUSSION

Here, we have described a patient with XLH and biopsy-proven HSCR who exhibited a nonsense mutation in exon 1 of the *L1CAM* gene, resulting in an extremely short protein devoid of the immunoglobulin domain that is essential for the molecule's heterophilic interactions with other proteins. Based on our observation of the phenotype and genotype of the propositus, we suggest that XLH-HSCR represents the severe end of the XLH spectrum, rather than a neomorphic mutation. In a review of the phenotypic spectrum of previously reported patients with XLH-HSCR and pathological mutations (Table I), the diagnosis was made in all patients based on severe structural abnormalities, such as severe hydrocephalus, dysplastic corpus callosum, and hypoplastic cerebellum. These observations further support the hypothesis that XLH-HSCR represents the severe end of the XLH spectrum. HSCR may occur in patients with other *L1CAM*-related features, such as agenesis of the corpus callosum, spasticity, or the absence of speech, without severe hydrocephalus and constipation. The review also revealed that infrequent features included micropenis, reported by Parisi et al. [2002]. Further confirmation in a large group of patients is needed to clarify whether this infrequent urogenital feature is related to the XLH spectrum. Yet another possibility includes the potential role of modifier genes and environmental factors.

The nonsense mutations previously reported in exons 13, 18, and 22 are likely to create transcripts susceptible to nonsense-mediated mRNA decay. Hence, the mRNA derived from these alleles will probably be reduced. In this situation, the total amount of partially functional protein is likely to be dependent on the efficiency of nonsense-mediated mRNA decay. Currently, the efficiency of nonsense-mediated mRNA decay is unpredictable based on the specific mutation type [Montfort et al., 2006]. Considering these factors, the validity of the proposed phenotype–genotype correlation or severe phenotype because of the extreme degree of protein truncation presented herein remains uncertain.

From a clinical standpoint, one should keep HSCR in mind when seeing patients with severe congenital hydrocephalus and constipation. A thorough abdominal investigation for HSCR may be warranted especially in the presence of adducted thumbs and severe congenital hydrocephalus with structural central nervous system abnormalities, such as dysplastic corpus callosum and hypoplasic cerebellum.

REFERENCES

Anderson RB, Turner KN, Nikonenko AG, Hemperly J, Schachner M, Young HM. 2006. The cell adhesion molecule l1 is required for chain migration of neural crest cells in the developing mouse gut. Gastroenterology 130:1221–1232.

Basel-Vanagaite L, Straussberg R, Friez MJ, Inbar D, Korenreich L, Shohat M, Schwartz CE. 2006. Expanding the phenotypic spectrum of L1CAM-associated disease. Clin Genet 69:414–419.

Bateman A, Jouet M, MacFarlane J, Du JS, Kenwrick S, Chothia C. 1996. Outline structure of the human L1 cell adhesion molecule and the sites where mutations cause neurological disorders. EMBO J 15:6050–6059.

Griseri P, Vos Y, Giorda R, Gimelli S, Beri S, Santamaria G, Mognato G, Hofstra RM, Gimelli G, Ceccherini I. 2009. Complex pathogenesis of Hirschsprung's disease in a patient with hydrocephalus, vesico-ureteral reflux and a balanced translocation t(3;17)(p12;q11). Eur J Hum Genet 17:483–490.

Jackson SR, Guner YS, Woo R, Randolph LM, Ford H, Shin CE. 2009. L1CAM mutation in association with X-linked hydrocephalus and Hirschsprung's disease. Pediatr Surg Int 25:823–825.

Jones KL. 2006. Smith's Recognizable Patterns of Human Malformation. Philadelphia, PA: Elsevier, Saunders. 202–203 p.

Kenwrick S, Watkins A, De Angelis E. 2000. Neural cell recognition molecule L1: Relating biological complexity to human disease mutations. Hum Mol Genet 9:879–886.

Montfort M, Chabas A, Vilageliu L, Grinberg D. 2006. Analysis of nonsense-mediated mRNA decay in mutant alleles identified in Spanish Gaucher disease patients. Blood Cells Mol Dis 36:46–52.

Nakakimura S, Sasaki F, Okada T, Arisue A, Cho K, Yoshino M, Kanemura Y, Yamasaki M, Todo S. 2008. Hirschsprung's disease, acrocallosal syndrome, and congenital hydrocephalus: Report of 2 patients and literature review. J Pediatr Surg 43:E13–E17.

Okamoto N, Wada Y, Goto M. 1997. Hydrocephalus and Hirschsprung's disease in a patient with a mutation of L1CAM. J Med Genet 34:670–671.

Okamoto N, Del Maestro R, Valero R, Monros E, Poo P, Kanemura Y, Yamasaki M. 2004. Hydrocephalus and Hirschsprung's disease with a mutation of L1CAM. J Hum Genet 49:334–337.

Parisi MA, Kapur RP, Neilson I, Hofstra RM, Holloway LW, Michaelis RC, Leppig KA. 2002. Hydrocephalus and intestinal aganglionosis: Is L1CAM a modifier gene in Hirschsprung disease? Am J Med Genet 108:51–56.

Vits L, Chitayat D, Van Camp G, Holden JJ, Fransen E, Willems PJ. 1998. Evidence for somatic and germline mosaicism in CRASH syndrome. Hum Mutat Suppl 1:S284–S287.

Yamasaki M, Thompson P, Lemmon V. 1997. CRASH syndrome: Mutations in L1CAM correlate with severity of the disease. Neuropediatrics 28:175–178.

nature genetics

Whole-genome sequencing of liver cancers identifies etiological influences on mutation patterns and recurrent mutations in chromatin regulators

Akihiro Fujimoto[1,16], Yasushi Totoki[2,16], Tetsuo Abe[1], Keith A Boroevich[1], Fumie Hosoda[2], Ha Hai Nguyen[1], Masayuki Aoki[1], Naoya Hosono[1], Michiaki Kubo[1], Fuyuki Miya[1], Yasuhito Arai[2], Hiroyuki Takahashi[2], Takuya Shirakihara[2], Masao Nagasaki[3], Tetsuo Shibuya[3], Kaoru Nakano[1], Kumiko Watanabe-Makino[1], Hiroko Tanaka[3], Hiromi Nakamura[2], Jun Kusuda[4], Hidenori Ojima[5], Kazuaki Shimada[6], Takuji Okusaka[7], Masaki Ueno[8], Yoshinobu Shigekawa[8], Yoshiiku Kawakami[9], Koji Arihiro[10], Hideki Ohdan[11], Kunihito Gotoh[12], Osamu Ishikawa[12], Shun-ichi Ariizumi[13], Masakazu Yamamoto[13], Terumasa Yamada[12], Kazuaki Chayama[1,9], Tomoo Kosuge[6], Hiroki Yamaue[8], Naoyuki Kamatani[1], Satoru Miyano[3], Hitoshi Nakagama[5,14], Yusuke Nakamura[1,15], Tatsuhiko Tsunoda[1], Tatsuhiro Shibata[2] & Hidewaki Nakagawa[1]

Hepatocellular carcinoma (HCC) is the third leading cause of cancer-related death worldwide. We sequenced and analyzed the whole genomes of 27 HCCs, 25 of which were associated with hepatitis B or C virus infections, including two sets of multicentric tumors. Although no common somatic mutations were identified in the multicentric tumor pairs, their whole-genome substitution patterns were similar, suggesting that these tumors developed from independent mutations, although their shared etiological backgrounds may have strongly influenced their somatic mutation patterns. Statistical and functional analyses yielded a list of recurrently mutated genes. Multiple chromatin regulators, including *ARID1A*, *ARID1B*, *ARID2*, *MLL* and *MLL3*, were mutated in ~50% of the tumors. Hepatitis B virus genome integration in the *TERT* locus was frequently observed in a high clonal proportion. Our whole-genome sequencing analysis of HCCs identified the influence of etiological background on somatic mutation patterns and subsequent carcinogenesis, as well as recurrent mutations in chromatin regulators in HCCs.

To gain insight into the molecular alterations of virus-associated HCC, we performed whole-genome sequencing (WGS) of 27 HCC tumors from 25 affected individuals, including two sets of multicentric tumors (MCTs) and matched normal lymphocytes (**Supplementary Table 1**). This included 11 hepatitis B virus (HBV)-related HCCs, 14 hepatitis C virus (HCV)-related HCCs and 2 HCCs without HBV or HCV infection (NBNC). Two affected individuals (HC3 and HC7) had two independent synchronous tumors, which were determined to be MCTs, not intrahepatic metastases, on the basis of their clinicopathological features. After PCR duplication removal, we obtained an average of 39.8× (tumor) and 32.7× (lymphocyte) coverage of the genomes by uniquely mapping 50–125 bp reads using paired-end sequencing (**Supplementary Fig. 1**). We identified somatic point mutations and indels with a false positive rate of less than 5% and 10%, respectively (**Supplementary Note**). We detected 4,886–24,147 somatic point mutations per tumor (**Fig. 1a** and **Supplementary Table 2**), and the average number of somatic point mutations at the whole-genome level was 4.2 per megabase. One tumor (HC11), which exhibited an exceptionally large number of somatic mutations (24,147 substitutions with predominant C>T/G>A transition at CpGs and 8,950 indels; **Fig. 1a**), was determined to have a DNA mismatch-repair defect due to a somatic nonsense mutation (encoding p.Glu234*) in *MLH1*. Analysis of the ratio of the depth of coverage identified 294 deleted regions ($\log_2$R ratio ≤ -1) and 20 amplified regions ($\log_2$R ratio ≥ 2) (**Supplementary Table 3** and **Supplementary Note**). Inconsistencies in mapped reads and subsequent PCR validation identified an average

[1]Center for Genomic Medicine, RIKEN, Yokohama, Japan. [2]Division of Cancer Genomics, National Cancer Center Research Institute, Tokyo, Japan. [3]Laboratory of DNA Informatics Analysis, Human Genome Center, Institute of Medical Science, The University of Tokyo, Tokyo, Japan. [4]National Institute of Biomedical Innovation, Ibaraki, Osaka, Japan. [5]Division of Molecular Pathology, National Cancer Center Research Institute, Tokyo, Japan. [6]Hepatobiliary and Pancreatic Surgery Division, National Cancer Center Hospital, Tokyo, Japan. [7]Hepatobiliary and Pancreatic Oncology Division, National Cancer Center Hospital, Tokyo, Japan. [8]Department of Gastroenterological Surgery, Wakayama Medical University, Wakayama, Japan. [9]Department of Medicine & Molecular Science, Hiroshima University School of Medicine, Hiroshima, Japan. [10]Department of Gastroenterological Surgery, Hiroshima University School of Medicine, Hiroshima, Japan. [11]Department of Anatomical Pathology, Hiroshima University School of Medicine, Hiroshima, Japan. [12]Department of Surgery, Osaka Medical Center for Cancer and Cardiovascular Diseases, Osaka, Japan. [13]Department of Gastroenterological Surgery, Tokyo Women's Medical University, Tokyo, Japan. [14]Division of Cancer Development System, National Cancer Center Research Institute, Tokyo, Japan. [15]Laboratory of Molecular Medicine, Human Genome Center, Institute of Medical Science, The University of Tokyo, Tokyo, Japan. [16]These authors contributed equally to this work. Correspondence should be addressed to H. Nakagawa (hidewaki@ims.u-tokyo.ac.jp) or T. Shibata (tashibat@ncc.go.jp).

Received 17 January; accepted 30 April; published online 27 May 2012; doi:10.1038/ng.2291

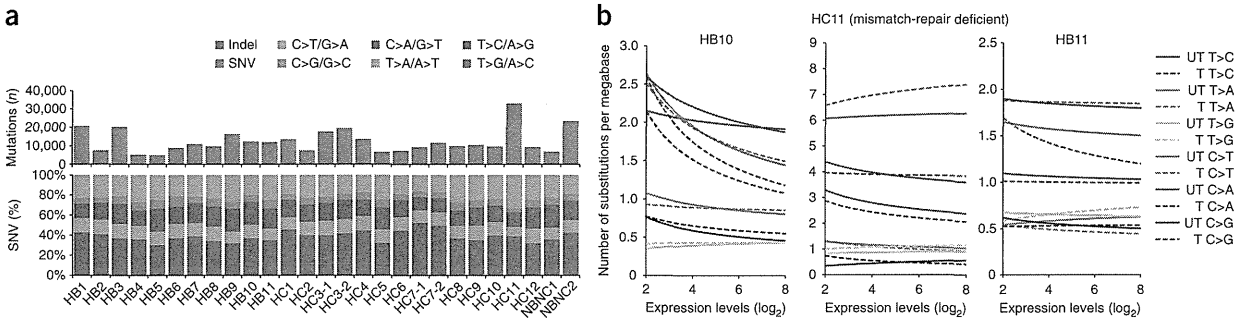

Figure 1 Somatic substitution patterns of HCCs. (**a**) The number of somatic substitutions and indels (top) and somatic substitution patterns (bottom) of the 27 HCC genomes. (**b**) Repair on the transcribed strand. Fitted curves show the effect of gene expression and strand bias on substitution prevalence. We used Agilent microarray expression data (Whole Human Genome 8 × 60K Oligonucleotide Microarray) in this transcription-coupled repair (TCR) analysis, and expression level indicates Agilent microarray intensity level units with a $\log_2$ scale. UT, untranscribed strands; T, transcribed strands.

of 20.8 genomic rearrangements per tumor (**Supplementary Table 4** and **Supplementary Note**). The number of somatic substitutions, indels and rearrangements were not significantly different between HBV- and HCV-related HCCs (**Supplementary Fig. 2**).

The distribution of somatic substitutions in HCC genomes is significantly deviated from the assumption of a uniform mutation rate (χ-square test; P value $< 1 \times 10^{-300}$), and we identified a dominance of T>C/A>G transitions (odds ratio (OR) = 2.02, 95% confidence interval (CI) = 1.95–2.08; **Fig. 1a**), as described previously[1], as well as C>A/G>T transversions (OR = 1.43, 95% CI = 1.36–1.50) and C>T/G>A transitions (OR = 1.75, 95% CI = 1.68–1.82), particularly at CpG sites (OR = 4.55, 95% CI = 4.30–4.80) (**Supplementary Fig. 3**). As C>T/G>A transitions are also dominant in other cancers[2], T>C/A>G transitions and C>A/G>T transversions could be characteristic mutational signatures of HCC genomes.

To examine the influence of transcription-coupled repair, we compared gene expression levels (**Supplementary Tables 5** and **6**) and the number of substitutions in seven HCCs. Only T>C and C>A changes but not C>T changes were effectively repaired on the transcribed strand (**Supplementary Fig. 4a–c**), and these repairs occurred more frequently in highly expressing genes (HB10 in **Fig. 1b** and **Supplementary Fig. 5**). Of note, transcription-coupled repair did not occur in the mismatch repair–deficient tumor with *MLH1* inactivation (HC11 in **Fig. 1b**). Another case (HB11) had a familial disposition to cancer (**Supplementary Table 1**) and exhibited a distinct mutation signature (increased indels, less dominance of T>C/A>G transitions and a decreased effect of transcription-coupled repair at T>C transitions) (**Fig. 1a,b**), although no causal mutation explaining the DNA-repair deficiency was identified. These findings suggest that transcription-coupled repair preferentially repairs somatic substitutions that are specifically increased in cancer.

One of the characteristic features of HCC is multiple occurrences or MCTs in a strong carcinogenetic background. First, we compared somatic mutation sites of the two pairs of MCTs (HC3 and HC7). In protein-coding regions, no common somatic mutations were identified. *ATM*, *FSIP2* and *LRFN5* were mutated in both MCTs of HC3, but the locations of the mutations were different. In non-coding regions, WGS identified 30 and 37 common somatic point mutations and indels in the HC3 and HC7 pairs, respectively. However, most of these occurred in repetitive regions, and all candidates that could be analyzed by Sanger sequencing (n = 20) were found to be germline variants (**Supplementary Note**). We also found no common structural alterations in these MCTs (**Fig. 2a**). These findings suggest that these synchronous MCTs developed through an accumulation of a completely different set of genetic alterations. Second, we applied

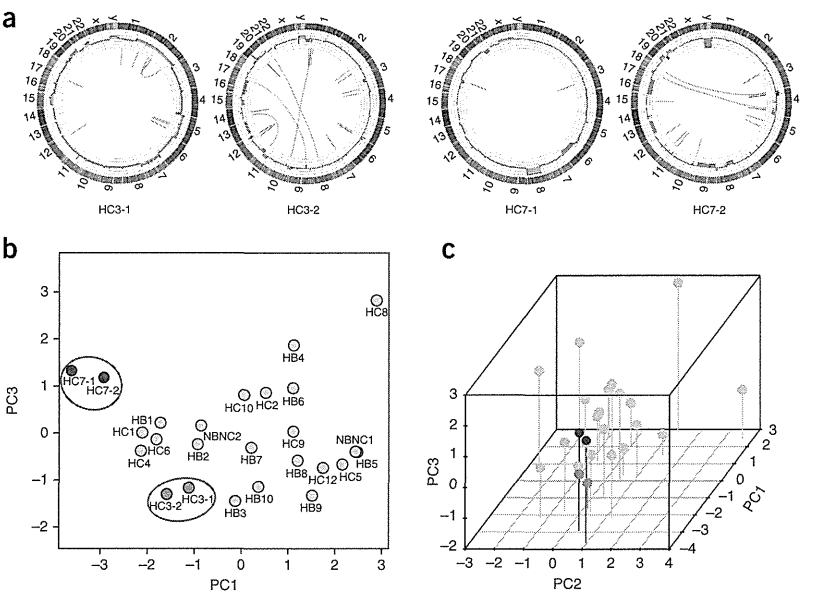

Figure 2 Mutation patterns of MCTs. (**a**) Circos plots[20] of the MCTs from two subjects (HC3 and HC7). Each circle plot represents validated rearrangements (inner arcs) and copy-number alternations (inner rings). In rearrangements, lines show translocations (green), deletions (blue), inversions (orange) and tandem duplications (red). Copy-number gain and loss regions are shown in green and red. (**b**) PCA of the somatic substitution patterns of 25 HCC genomes. Two sets of MCT pairs (HC3 and HC7) are shown by green and blue, respectively, and are circled in red. (**c**) Three-dimensional plot of principal components (PCs) for 25 HCCs on somatic substitution pattern. Two sets of MCT pairs (HC3 and HC7) are shown in green and blue, respectively.

Table 1 Significantly mutated genes and their mutation frequency in the validation set

Gene	Chr.	Start	End	CDS length (bp)	Coding indel	Missense	Nonsense	Splice site	Total	*P* value	*q* value	Frequency in validation set
TP53	17	7,572,927	7,579,912	1,218	0	11	0	3	14	0	0	NA
ERRFI1	1	8,073,270	8,075,679	1,397	1	0	2	0	3	0.00020	0.0034	3.1% (2/65)
ZIC3	X	136,648,851	136,652,229	1,412	0	3	0	0	3	0.00050	0.0041	3.3% (4/120)
CTNNB1	3	41,265,560	41,280,833	2,398	0	3	0	0	3	0.0015	0.0071	NA
GXYLT1	12	42,481,588	42,538,448	1,351	0	3	0	0	3	0.0013	0.0071	0.8% (1/120)
OTOP1	4	4,190,530	4,228,591	1,859	1	2	0	0	3	0.0015	0.0071	0.8% (1/120)
ALB	4	74,270,045	74,286,015	1,882	3	0	0	0	3	0.0022	0.0089	3.3% (4/120)
ATM	11	108,098,352	108,236,235	9,415	1	4	0	0	5	0.0037	0.013	5.0% (6/120)
ZNF226	19	44,674,234	44,681,827	2,424	1	1	1	0	3	0.0043	0.014	3.3% (4/120)
USP25	21	17,102,713	17,250,794	3,260	1	2	0	0	3	0.0051	0.015	0% (0/120)
WWP1	8	87,386,280	87,479,122	2,857	2	1	0	0	3	0.0060	0.016	7.7% (5/65)
IGSF10	3	151,154,477	151,176,497	7,892	0	4	0	0	4	0.0091	0.023	3.3% (4/120)
ARID1A	1	27,022,895	27,107,247	6,934	2	1	0	0	3	0.011	0.026	10% (12/120)
UBR3	2	170,684,018	170,938,353	5,819	0	3	0	0	3	0.018	0.041	0.8% (1/120)
BAZ2B	2	160,176,776	160,335,230	6,643	0	3	0	0	3	0.024	0.050	1.6% (2/120)

Significantly mutated genes with more than two mutations are shown. Chr., chromosome.

principal-component analysis (PCA) to further examine genome-wide somatic mutation patterns. Two HCCs (HC11 and HB11) exhibited quite distinct substitution patterns compared to the other samples due to their mismatch-repair deficiency (**Supplementary Fig. 6a**). Therefore, they were excluded from PCA. Notably, the pairs of each MCT (HC3 and HC7) were tightly clustered in PCA (permutation test; *P* value = 0.00050), indicating similar somatic substitution patterns on the whole-genome level (**Fig. 2b,c**). Considering that these MCTs shared the exact same genetic and environmental backgrounds, the somatic substitution patterns are likely to be determined by the etiological backgrounds in which the tumors developed.

We also examined associations between the principal components and clinical factors. Although the correlations between somatic substitution patterns and age at diagnosis, tumor grade, liver fibrosis and tumor size were not significant, habitual alcohol drinking and the occurrence of synchronous or metachronous multiple liver nodules showed significant association with principal components of the somatic substitution patterns (habitual alcohol drinking, $P = 0.028$; multiple liver nodules, $P = 0.016$) (**Supplementary Fig. 6b,c**). Virus type showed a marginal association with substitution pattern ($P = 0.091$) (**Supplementary Fig. 6d**). In addition to viral infection, alcohol abuse, obesity, diabetes and other metabolic disorders are also risk factors for liver carcinogenesis, and its background etiology is very heterogeneous[3]. Multiple background factors, including germline variants, epigenetic status of liver, virus infection, exposure to other environmental carcinogens, inflammation and a combination of these factors, would contribute to the somatic mutation pattern in cancer genomes.

Across all 27 HCC genomes, we detected a total of 2,048 (75.9 per tumor) protein-altering point mutations, including 1,734 missense mutations, 101 nonsense mutations, 161 short coding indels and 52 splice-site mutations (**Supplementary Table 2**). After adjusting for the regional deviation of somatic mutation rate and gene length, significantly frequent mutations were found to occur in 15 genes, with a false discovery rate (FDR) of ≤0.05 (**Table 1** and **Supplementary Table 7**). *TP53* and *CTNNB1* (encoding β-catenin) genes were significantly mutated in HCC, as previously reported[4]. Five mutations of *ATM* were detected in four tumors without *TP53* mutations. Sequencing analysis on an independent set of 120 HCCs detected 6 additional *ATM* mutations (5%) (**Table 1** and **Supplementary Table 8**). Three mutations of *ARID1A*, two frameshifts and one missense, were detected in three tumors by WGS. *ARID1A* encodes a key component of the SWI-SNF chromatin-remodeling complex, and *ARID1A* mutations have been detected in ovarian cancer[5] and many other cancers[6]. Sequencing analysis of the 120 HCCs detected 12 additional mutations of *ARID1A* (10%) (**Table 1** and **Supplementary Table 8**). WGS detected three somatic mutations in *ERRFI1*, two nonsense and one frameshift, in two tumors. *ERRFI1* encodes a protein that inhibits the kinase domains of EGFR and ERBB2 (ref. 7), and *Errfi1* knockout mice showed enhanced hepatocyte proliferation[8]. These mutations may cause the loss of inhibitory function and thereby activate the EGFR signaling pathway in HCC. We detected 2 additional mutations of *ERRFI1* (3.1%) in 65 independent HCCs (**Table 1** and **Supplementary Table 8**). Three

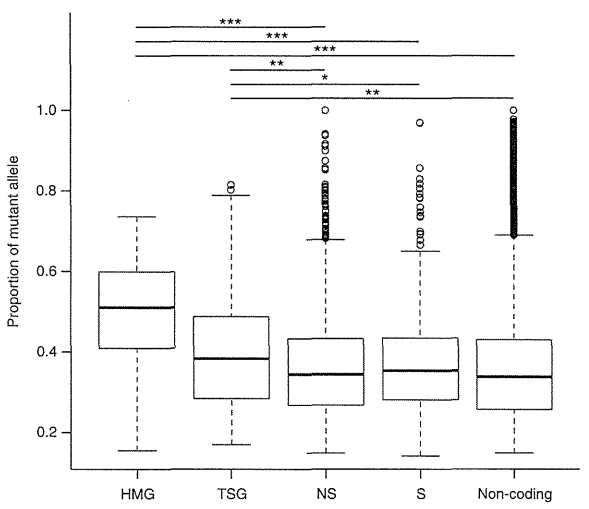

Figure 3 Mutant allele proportions of point mutations. HMG, highly mutated genes, genes whose mutation frequency was greater than 3% in the validation set (*ARID1A, IGSF10, ATM, ZNF226, ZIC3, WWP1* and *ERRFI1*); TSG, known tumor suppressor genes annotated by MutationAssessor[21]; NS, nonsynonymous; S, synonymous. Non-coding includes point mutations in non-coding regions except for in splice sites. The edges of the boxes represent the 25th and 75th percentile values. The whiskers represent the most extreme data points, which are no more than 1.5 times the interquartile range from the boxes. $*P < 0.05$; $**P < 0.01$; $***P < 0.001$.